

Multilayers of Carbodithioate and Sulfide-Linked CdSe

Nanocrystals: Progressive Increasing of Exciton Delocalization

B. Vercelli^{a*}, T. Virgili^{*b}, M. Pasini^c, A. Berlin^d, G. Zotti^e

^aIstituto di Chimica della Materia Condensata e di Tecnologie per l'Energia – CNR-ICMATE Milano, Via Cozzi, 54 – 20125 Milano (Italy).

^bIstituto di Fotonica e Nanotecnologie – CNR-IFN, P.zza Leonardo da Vinci, 32 – 20132 Milano (Italy).

^cIstituto per lo Studio delle Macromolecole – CNR-ISMAL, Via Alfonso Corti, 12 – 20133 Milano (Italy).

^dIstituto di Scienze e Tecnologie Molecolari – CNR-ISTM, Via Golgi 19 – 20133 Milano (Italy).

^eIstituto di Chimica della Materia Condensata e di Tecnologie per l'Energia – CNR-ICMATE, C.so Stati Uniti, 4 – 27135 Padova (Italy).

ABSTRACT: Multilayers of sulphur-based anchoring group linkers and CdSe nanocrystals (NCs) were realized on ITO substrate via layer-by-layer alternation. The materials were investigated by UV-vis and FTIR spectroscopy, photoluminescence and photoconductivity. We found that the change of NCs packing during the multilayers build-up produces a progressive increase of exciton delocalization. In fact during multilayer deposition the NCs first excitonic peak shifts progressively towards longer wavelengths. We found a linear relation between the optical band gap shift (ΔE_{gn}) and the inverse of number of CdSe-NCs layers (n) for $n > 2$, in particular the decrease of its value for the infinite multilayer from the one of the solution (2.10 eV) goes from 18 meV for the 1,2-ethylene-bis(dithiocarbamate) (EDTC) linker to 66 meV for sulphide dianions, corresponding to an apparent increase of the exciton radius of 0.20 nm and 0.85 nm, respectively.

INTRODUCTION

Semiconductor nanocrystals (NCs) are challenging materials to be exploited in devices like light emitting diodes, solar cells and photodetectors, because of their unique electronic, magnetic and optical properties. Typically such devices require that the NCs should be both distinct particles that exhibit quantum confinement of the charge carriers and strongly coupled to the neighbouring particles when they are assembled into a film. In fact, quantum confinement allows the electronic properties to be tuned with the size, while electronic coupling facilitates charge transport in the device. Unfortunately, such goals are difficult to achieve because of the very poor inter-particles contacts caused by linkers between NCs¹. In fact, though much effort has been devoted in optimizing molecular core conductivity, there have been relatively few attempts at designing optimal anchoring groups to semiconducting nanocrystals. In a previous work we found that multilayered hybrid films realized by the alternation of CdSe-NCs and bi-functionalized linkers bearing dithiocarbamate moiety with ethylene or phenylene as spacers (EDTC and PDTC, respectively in Chart 1), have shown promising photoconductive properties², which were supported by photo-excited carrier dynamic experiments combined with theoretical calculations³. These latter studies show that the dithiocarbamate anchoring

group causes the hybridization of the molecular HOMO state with the CdSe-NCs layers, which may favor the delocalization of the charge carriers through the layers. So it was supposed that other sulfur-based anchoring groups linkers (S-linkers) may produce similar effects and, among them, the carbodithioate (CDT) moiety was found of particular interest⁴.

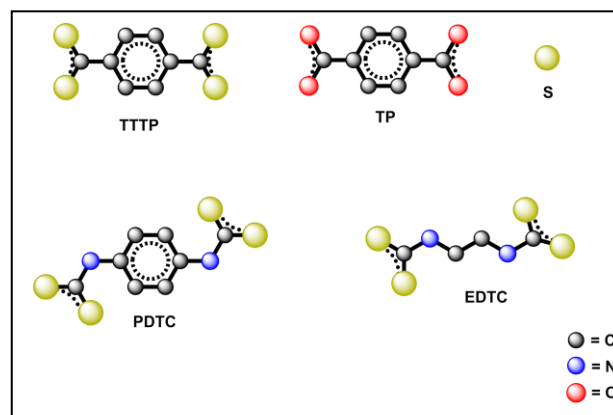


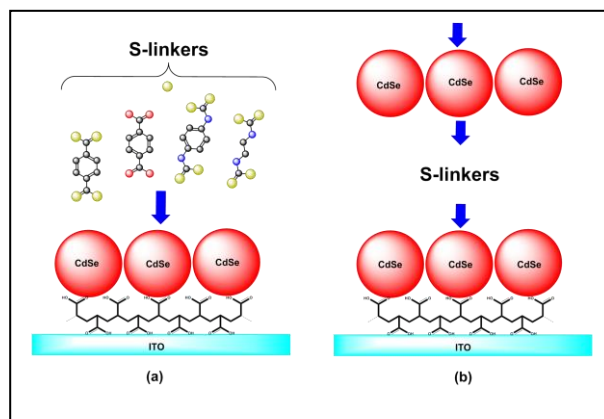
Chart 1. – S-linkers structures and the structure of terephthalate dianion (TP) employed for comparison.

In fact, single-molecule conductances⁵ of CDT-based conjugated systems bridged to gold electrodes, demonstrate that the CDT-moiety favours electronic coupling to the metal electrode and lowers the effective barrier for charge transport with respect to thiol linkers. The results were supported by DFT calculations⁶. Films based on gold nanoparticles interlinked by bis-carbodithioate derivatives have shown improved optical and conductive properties⁷ and CDT-based systems were also employed as linkers for CdSe-NCs⁸⁻¹⁰.

Among CDT-based linkers tetrathioterephthalate (TTTP) dianion (Chart 1) could be of particular interest, because, it is both a bis-bidentate chelating linker and is coplanar with a relatively short C-C distance between C₆H₄ and -CS₂⁻ moieties¹¹, favouring conjugation along the molecule-backbone. Moreover, recent studies on the synthesis of TTTP-based polymers⁹ and dimers¹⁰ have shown that these materials contributed to the development of metal-organic solids whose electronic properties are comparable to those of pure inorganic chalcogenide-based materials. TTTP has a low absorption energy, which is at 590 nm for the dianion⁹ and shifts to ca 660 nm for its zinc complex⁹. The energy gap of TTTP zinc-complex (1.9 eV) is comparable with the one of commonly used CdSe-NCs (e. g. 2 eV for a 5 nm diameter NCs), suggesting that the photo-physical properties of the TTTP-based CdSe-NCs system could be enhanced.

Another interesting S-linker could be the sulphide ion whose atomic dimensions are expected to favour charge carriers delocalization in multilayered films through the substitution of NCs native ligands and the reduction the distance among NCs. Recently, a variety of small anions like halides¹¹ and chalcogenides¹²⁻¹⁴, were employed to increase the electronic coupling among NCs. Sulphide salts are cheap, stable and are known to form colloidal dispersions of sulphide-capped NCs in polar solvents^{13, 14}. Sulphide ion was also employed as capping ligand in devices build up¹⁵ and it is expected to be successfully employed as “linker” in the layer-by-layer (LBL) growing of multilayered CdSe-NCs hybrid films.

In the light of the above considerations, in the present work the S-linkers TTTP and sulphide dianions were employed in comparison with the previously investigated bis-dithiocarbamate PDTC and EDTC ones (Chart 1) for the realization and characterization of multilayered hybrid films (Scheme 1b). The study provides the determination of the electronic properties of the linkers by means of both UV-vis and electrochemical analyses. Linkers coordination to CdSe-NCs surface was investigated in bulk by FTIR analyses and in monolayers by UV-vis and electrochemical determinations. 10-multilayered film formation was monitored with UV-vis spectroscopy and it was observed a decrease of the energy of the optical band-gap (ΔE_{gn}) which depends linearly with the inverse of the number of layers (n). The change of NCs packing during multilayers build-up causes progressive increase of exciton delocalization. The effect was modelled and discussed in the light of the photoluminescence and photoconductive properties of the multilayers.



Scheme 1. – (a) Ligand exchange in monolayer; (b) Multilayer build-up

RESULTS AND DISCUSSION

Linkers – S-linkers electronic properties were determined in solution by optical and electrochemical investigations as follows.

UV-vis analysis - The electronic spectrum of TTTP shows a low intensity peak ($\epsilon = 10^3 \text{ M}^{-1} \text{ cm}^{-1}$, in acetonitrile) at 530 nm (Fig. S1 and Table 1), which originates from the $n\text{-}\pi^*$ transition of the -CS₂⁻ chromophore⁹ and a second peak at 330 nm ($\epsilon = 10^4 \text{ M}^{-1} \text{ cm}^{-1}$, in acetonitrile), which is assigned to the $\pi\text{-}\pi^*$ transition. A comparison with the electronic spectrum of terephthalate dianion (TP, Chart 1), the TTTP molecule with oxygen in place sulphur, was performed to study the effect of sulphur on TTTP energy levels. TP electronic spectrum shows only a shoulder at 270 nm (Fig. S1, Table 1) due to an analogous $\pi\text{-}\pi^*$ transition. In fact, the C-S π -bonds are weaker than the C-O ones so they cause a decrease of TTTP LUMO energy level. On the other hand sulphur is less electronegative than oxygen causing an increase of TTTP HOMO one. As a consequence the onset optical gap of TTTP (1.90 eV, Table 1) is lower than the one of TP (4.6 eV, Table 1). The electronic spectrum (Fig. S1) of PDTC, the corresponding N -spaced form of TTTP, presents only an absorption peak at 307 nm ($\epsilon = 2 \times 10^4 \text{ M}^{-1} \text{ cm}^{-1}$, in MeOH) assigned to a $\pi\text{-}\pi^*$ transition and corresponding to an optical gap of 3.30 eV, Table 1. EDTC UV-vis analyses are difficult to perform because its maximum is at higher energies.

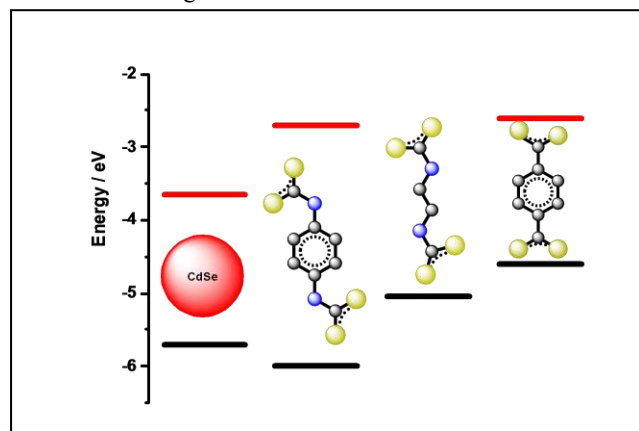
Table 1. - Oxidation and reduction peak potentials vs Ag/Ag⁺ (E_p), optical λ_{max} and optical gap E_g for CdSe-NC and S-linkers dianions.

	$E_{p\text{ox}} / \text{V}$	$E_{p\text{red}} / \text{V}$	$\lambda_{\text{max}} / \text{nm}$	E_g / eV
TTTP	-0.35	-2.30	530, 330	1.95
TP	-	-	270	4.60
PDTC	1.20	-	340(sh), 307	3.30
EDTC	0.25	-	-	-
CdSe (4.5nm)	0.80	-	597	2.08

Electrochemistry - TTTP is both oxidized and reduced in the accessible potential range. Its oxidation (Fig. S2) is a one-electron irreversible process at -0.35 V, while its reduction is a two-electron reversible process at -2.30 V (Table 1). The cor-

responding electrochemical gap is 1.95 eV, in very good agreement with the above reported optical onset value in solution¹⁶. TTTP oxidation, whose cyclic voltammetric (CV) profile (Fig. S3) resembles the one reported for dithiolates, for example, 2,5-dimercapto-1,3,4-thiadiazole dianin¹⁶, leads to the formation of the dimer (A in Fig. S3) and then of the polymer (B in Fig. S3). TTTP reduction should produce the 7,7,8,8-quinodimethane tetrathiolate tetra-anion, which resembles the thiolate-based tetra-anions present in thiolate-based polymers¹⁷⁻¹⁹. EDTC and PDTC show one-electron oxidation processes (Fig. S2 and Table 1) and their peak potential values are 0.6 V and 1.55 V, respectively more positive than TTTP one. No reduction responses were observed for both molecules.

In Scheme 2 are reported the HOMO and LUMO energy levels of the S-linkers¹ calculated from the above reported optical and the electrochemical results and which will be deeply treated in the following.



Scheme 2. – Diagram showing the energy levels of CdSe-NCs (4.5 nm), PDTC, EDTC and TTTP.

CdSe-Linkers Systems

We employed soluble CdSe-NCs with the surface capped by native ligands hexadecylamine (HDA) and stearic acid (SA) and with an absorption maximum around 600 nm, corresponding to an average size of 4.5 nm (see the Experimental for more details). The occurrence of linkers coordination to CdSe-NCs surface was studied in bulk by FTIR spectroscopy, while in monolayers (Scheme 1a) by UV-vis and electrochemical analyses.

Bulk Structures – FTIR analyses - The occurrence of coordination of TTTP and sulphide-ion linkers to CdSe-NCs was evaluated by reacting CdSe-NCs CH₃Cl solutions with TTTP solu-

¹HOMO energy levels were determined from the electrochemical S-linkers oxidation peak potential according to $E_{HOMO} = -(4.39 + 0.34 + E_{ox})$, where E_{ox} is S-linker oxidation peak potential vs Ag/Ag⁺ electrode (0.34 V vs SCE), while LUMO energy levels were obtained by the difference between the optical energy gap and the HOMO values. EDTC LUMO level is not reported in Scheme 2 because of difficulties in determining both its optical energy gap and its reduction peak potential.

tions in EtOH or sulphide in H₂O/MeOH mixtures in 1:1 v/v ratio. The FTIR spectra, Fig.S4, show that hexadecylamine bands at 3300 and 1640 cm⁻¹ disappear after sulphide ion lig-

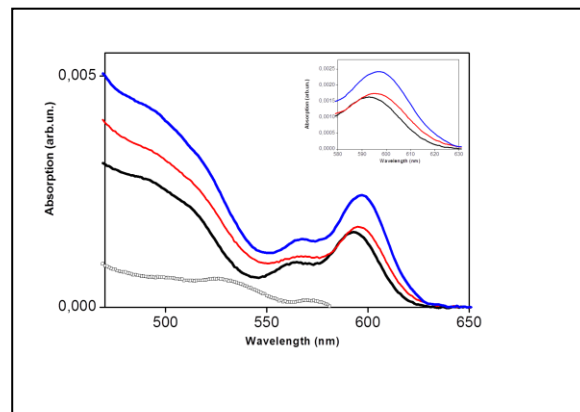


Figure 1. – UV-vis absorption spectra of CdSe-NCs monolayer with: external native ligands (black line), TTTP coordinated (red line), sulphide ion coordinated (blue line) and contribution TTTP resulted by the subtraction from the red line of the black line (black line + symbols). In the inset, zoom of the spectra at around 600 nm

and-exchange and the C-H stretching bands (at 2930 cm⁻¹ and 2850 cm⁻¹) of hexadecylamine and stearic acid decrease of ca 20 fold. This behavior in agreement with reported data supports the ability of the sulfide ion to replace different kind of CdSe-NCs organic capping molecules, like amines, carboxylates, phosphonic acids, etc.¹³

The coordination of TTTP to NCs surface is revealed by the substitution of the NCs native ligands, as in the sulfide ion case, and by the presence of the typical C=S stretching bands of TTTP at 1207 cm⁻¹ and 1019 cm⁻¹ (Fig. S5). These FTIR bands are shifted bathochromically of 28 cm⁻¹ if compared with the ones of un-coordinated TTTP salt, suggesting the strong coordination of TTTP to the NCs surface. The same ligand substitution was observed also with PDTC and EDTC linkers². The observed (Fig. S4 and S5) persistence of CH₂ stretching bands around 2900 cm⁻¹ suggests that the native ligands are to some extent kept in bulk systems. This is not the case with the mono-multilayers reported below, where the extensive surface native ligand substitution takes place^{2 and references therein}.

Monolayers - UV-vis analysis – The electronic spectra of CdSe-NCs monolayers with external native ligands, (CdSe-NL, Fig. 1 black line and Scheme 1a) show the dominant CdSe absorption bands at around 600 nm, 560 nm and 500 nm which correspond to its exciton bands^{20, 21}. In the case of TTTP coordination (Fig. 1 red line, Scheme 1a) the spectrum shows the presence of a new band at around 530 nm highlighted by the difference between the two spectra (see line + symbols in Fig. 1) due to the above described n-π* transition of the ligand (see Figure S1). Moreover a small bathochromic shift of around 2 nm of the first-exciton peak at 600 nm is shown. From the intensity of the TTTP band we estimate a linker coverage value of ca 1 × 10⁻⁹ mol cm⁻², in agreement with the previously reported data^{2, 22, 23} and corresponding to a

dense coverage (CdSe/TTTP molar ratio of ca 10). Sulfide-ion coordination cannot be detected by specific absorption peaks in the UV-vis spectrum, but a red-shift of 5 nm of the main peak is present (Fig. 1 blue line and S6) which will be deeply discussed in the following, together with the ones of TTTP, PDTC and EDTC linkers. The UV-vis spectra of PDTC and EDTC on CdSe-NCs monolayers were previously reported².

Electrochemistry – To better understand the electrochemistry of S-linkers coordinated to CdSe-NCs monolayers surface (Scheme 1a) a short discussion on the effect of EtOH treatment on the electrochemical oxidative response of CdSe-NL monolayers should be done. In fact it is well known that CdSe-NL monolayers undergo in organic medium a sharp and irreversible oxidation process at 1.3 V vs Ag/Ag⁺ (Fig. S7) due to selenide oxidation and corresponding to the passage of two electrons per CdSe unit²². After EtOH treatment of the monolayers the signal splits into two peaks namely: A at 0.80 V and B at 1.30V (Fig. S7). FTIR spectra (Fig. S8) of the CdSe-NL bulk material after EtOH treatment show a partial removal of native ligands (NL) from NCs surface. This partial NCs surface coverage observed upon EtOH treatment is supposed to promote an efficient solvent wetting of CdSe-NL monolayers surface during the oxidative process, which causes firstly the oxidation of the surface CdSe units, un-blocked from NL (peak A) and then of the core counterparts (peak B)²². This peaks assignment is confirmed by the matching between the experimental charge distribution between peaks A and B (ca 0.54) and the theoretical one estimated on a simple geometrical basis (0.5). It was also observed that the sum of the integrated charges of peaks A and B equals the one of the untreated CdSe-NL monolayers and the CV response is independent from the scan rate in the range of 3-100 mV s⁻¹ meaning that there is no dynamic conversion from B to A forms in the used time scale of analysis. Moreover, peak A corresponds to a HOMO energy level value of ca -5.6 eV, which is in good agreement with the one reported for CdSe-NCs of 4.5 nm of diameter (-5.7 eV), while the 0.5 V more positive peak B is at the same potential value as the peak of EtOH un-treated CdSe-NL monolayers. No reduction processes are observed for CdSe-NL monolayers, also upon EtOH treatment, down to -2.20 V, which is the ITO electrochemical stability limit. We found that sulfide ion, EDTC and PDTC linkers surface coordination to CdSe-NCs monolayers does not affect their electrochemical responses. In fact, the oxidation shows the same CV shape (Fig. S9) of the above described CdSe-NL monolayers treated with EtOH, while the reduction shows no signals down to -2.20 V.

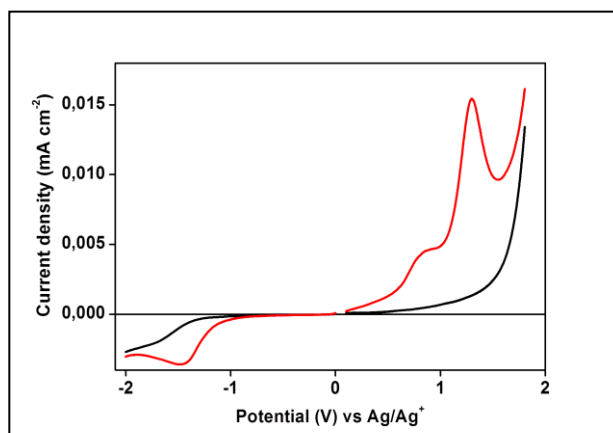
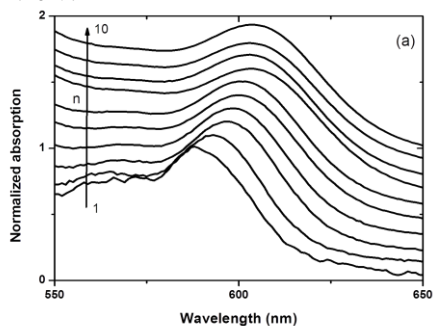


Figure 2. – Cyclic voltammograms in acetonitrile + 0.1 M TBAP of bare ITO (black line) and CdSe-TTTP (red line). ITO (2 cm²), $\nu = 0.02 \text{ V s}^{-1}$.

It is interesting to note that TTTP linker surface coordination to CdSe-NCs monolayers affects their reduction electrochemical response. In fact, Fig. 2 shows a peak at -1.45 V, which is not present with the other S-linkers and is ca 0.8 V less negative than the above observed TTTP reduction peak potential in solution (see Table 1 and Fig. S3).

This TTTP peak potential value in monolayers may be ascribed to the charge delocalization of TTTP outer dianion units induced by the coordination to Cd²⁺ ions on NCs surface. From the integrated reduction charge, which is ca 20 % of the CdSe-NCs oxidation one, we obtained a CdSe/TTTP molar ratio of ca 5, which is in reasonable agreement with the above reported optical datum.

Multilayers – Multilayered films (Scheme 1b) are built by the alternate exposure to linker solutions and CdSe-NCs dispersions in organic solvent (see experimental section for details). The ligand exchange carried out at room temperature for some minutes on the layered CdSe-NCs leads to a quantitative replacement of the native surface ligands²². Multilayers appear robust enough to tolerate a standard sticky-tape test with no appreciable loss. UV-visible spectroscopy was used to monitor the assembling process of the films on ITO substrates. CdSe absorbance (at ca 600 nm, CdSe first exciton band) increases linearly with the number of layers for all the employed S-linkers, showing a stepwise and uniform assembly process (the multilayer growth with sulfide ion in Fig. 3 is reported as example). Note that the first layer is not ligand exchanged (Schemes 1a and 1b).

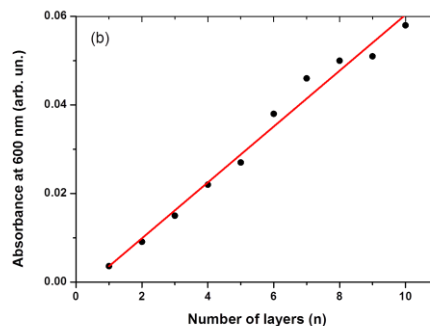


Figure 3. – (a) Normalized UV-vis spectra with vertical off-set of ITO/PAAH/(CdSe/S)_{n-1}/CdSe (CdSe-S) multilayers (n = 1–10) and (b) CdSe absorbance value (at 600 nm) vs number of layers. Spectra are background-corrected.

The two-side absorbance differential increase (ΔA_{CdSe}) is ca 6×10^{-3} au layer⁻¹ (corresponding to ca. 1×10^{-8} mol cm⁻² layer⁻¹ in CdSe units²⁴) for all the employed S-linkers. This coverage value is ca 60% of the one reported² for PDTC and EDTC-based multilayers and, according to a previous work²² is accounted for the small dimensions of the actually employed NCs (4.5 nm of diameter instead of 7.5 nm).

Thickness analysis has given results compatible with well-packed structures. Multilayers display a differential thickness of 3.5 nm layer⁻¹ and for all the structures the ratio of the differential thickness and NCs diameter is around 0.8, i.e., very close to the ideal value ($\frac{\sqrt{3}}{3}$) for a regular 3D hexagonal close-packed structure of NCs²².

Moreover, multilayers growth with S-linkers show an increase of the band-edge shift with the increasing number of layers n (Fig. 3), which will be deeply analyzed in the following. We, also, observed a slight peak broadening passing from the 1st to the 10th layer both in the Sulfur-based multilayers and in the TP-based ones (Fig. S10), probably ascribed to solid-state effects (i.e. NC-NC interaction).

Photoconductivity – Under the applied conditions the S-linker-based multilayers display photocurrent transients with a response time of some seconds (Fig. S11) not shown by cast films of the original CdSe-NCs of comparable thickness. The response is stable for several minutes and at least 5-10 on-off cycles. Surprisingly, sulphide ion-based multilayers photocurrents are comparable with the ones reported for PAAH-based multilayers (bearing carboxylate functional groups)²³ and 10 and 100 fold lower respectively than EDTC and PDTC-based ones whereas the small dimensions of sulphide ion are supposed to favour a strong interaction among NCs and enhance the charge transfer. On the other side, in agreement with the PL data (Fig. S12 and SI for more details), photocurrent responses of TTTP-based multilayers are 100 times lower than the ones of sulphide ion-based multilayers.

UV-vis spectra of CdSe-NL monolayers, show that the surface coordination of the S-linkers causes a bathochromic shift of the main absorption peak of CdSe-NL monolayers. In particular, sulphur ion coordination causes the largest shift of 5 nm (inset Fig. 1 and Fig. S6), corresponding to 17 meV, while PDTC, TTTP and EDTC linkers present 14 meV, 8 meV and 2 meV shifts, respectively. Such shifts were not observed with the larger 7.5 nm diameter NCs employed in previous work² and are typical of S-linkers. In fact, the coordination of TP linker (employed in this study only for comparison) does not cause any peak shift (Fig. S10).

In the case of sulphide ion the effect may be ascribed to an apparent NCs diameter increase induced by the external sulfide layer which makes CdSe-NCs much similar to core-shell CdSe@CdS-NCs, besides no significant changes are reported to occur in the size or shape of the CdSe-NCs upon sulfide coordination^{25,26}. Moreover, Weiss^{27,28} observed the same phenomenon in solution upon phenyldithiocarbamate (PTC) linker coordination to CdSe-NCs. Weiss found that the observed shifts corresponds to an apparent increase of NCs excitonic radius of 0.26 nm which may suggest that PTC decreases the NCs energy gap by a progressive exciton delocalization through the ligand shell; the data were also supported by DFT calculations^{27,28}. In agreement with our findings, the phenomenon resulted typical of linkers bearing sulphur-based anchoring groups (i.e. ditiocarbamate)²⁹.

Passing from CdSe-NCs monolayers to multilayers, the UV-vis spectra show a progressive bathochromic shift of CdSe-NCs main absorption peak during the multilayer formation with S-linkers (Fig. 3a and Fig. 4a). For 10 layers systems the shift corresponds to 53 meV for the sulphide-based, 31 meV for the PDTC-based, 14 meV for the TTTP-based and 10 meV for EDTC-based. For the TP-based is null (Fig. S10) confirming, in agreement with the above reported data on monolayers, that the phenomenon is typical of the S-linkers.

Following the hypothesis of Weiss developed for monolayers we extended the same model to multilayers. We described the red shift as a progressive increase of the excitonic radius ΔR (Table 2) and we found that for the largest shift observed in sulphide-based systems we have an increase of the excitonic radius (corresponding to an increase of the exciton delocalization) of about 0.65 nm³⁰.

To understand this behaviour we started by considering that the multilayers build-up induces an extended conjugation of the exciton. So we define the observed bathochromic optical shift of the NCs n -layer ΔE_{gn} as:

$$\Delta E_{gn} = E_{NC} - E_{gn}$$

where E_{NC} is the energy gap of the CdSe-NCs solution (or of its first NCs layer on PAAH-primed ITO, E_{g1}) and E_{gn} is the energy gap of the NCs n -layer.

Then we modelled the ΔE_{gn} as a function of the number of layers n , in a one-dimensional case, like along the chain length in polyconjugated systems³¹, as follows (see SI for details):

$$\Delta E_{gn} = A - \frac{B}{n} \quad (1)$$

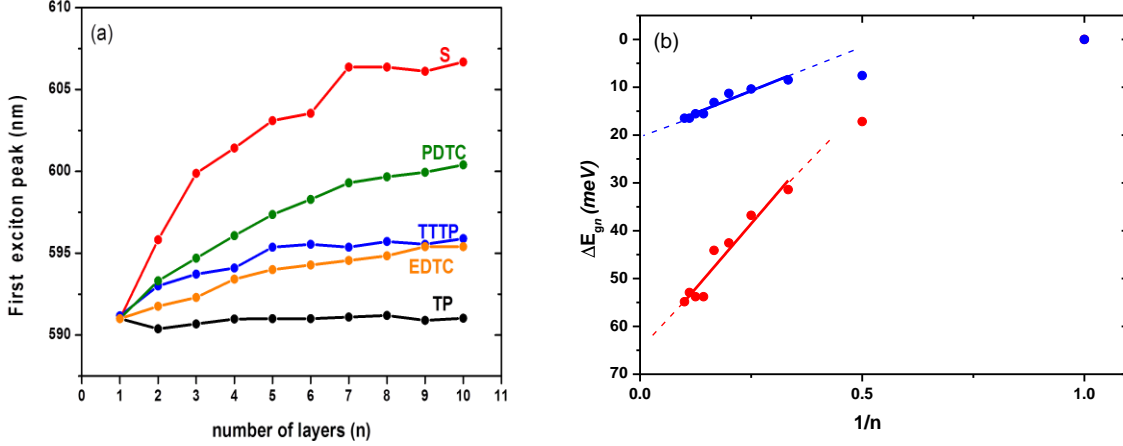


Figure 4. – (a) Relevant plot of CdSe-NCs first exciton peak wavelength vs number of layers of CdSe-X linkers (b) Relevant plot of CdSe-NCs band edge shift (ΔE_{gn}) vs the inverse of the number of layers ($1/n$) of CdSe-S (red line) and CdSe-TTTP (blue line) multilayers.

Table 2. - Intercept and slope for the ΔE_{gn} vs $1/n$ linear relationship for S-linkers-based CdSe-NCs n -multilayers ($\Delta E_{gn} = A - \frac{B}{n} = \Delta E_{\infty n} - \frac{k\Delta E_{\infty n}}{n}$); $k = B/\Delta E_{\infty n}$). The apparent increase of the excitonic radius ΔR is also reported [31].

	$\Delta E_{\infty n}$ / meV	B / meV	k / meV	ΔR / nm
CdSe-S	66	108	1.7	0.85
CdSe-PDTC	48	85	1.8	0.59
CdSe-TTTP	20	38	1.9	0.23
CdSe-EDTC	18	45	2.5	0.20

where A is the energy of bathochromic shift at infinite multilayer $\Delta E_{g\infty}$, which describes the progressive exciton delocalization along an extensive one-dimensional vertical conjugation through the layers. In table 2, where the results of our fitting are reported, the coefficients B and A of equation (1) are proportional as follows: $B = kA$.

So we can write Equation (1) as:

$$\Delta E_{gn} = \Delta E_{g\infty} - \frac{k\Delta E_{g\infty}}{n} \quad (2)$$

which resembles a multilayer power law model^{32,33}, see SI for details.

Fig. 4b shows that equation 2 holds for $n > 2$, in fact the first and the second layers deviate from linearity. The k values reported in table 2 are higher than the expected value of 1^{32,33}, suggesting that in our multilayered systems the progressive exciton delocalization through the layers can be described as a combination of an extended conjugation along the vertical direction and of a statistical contribution coming from components that are not vertically oriented. In fact, NCs size (ca 4.5 nm) is supposed to allow a partial random orientation of the linkers whose maximum component, however, is still along the layer normal. So, our multilayered systems may be intend-

ed as a $n-2$ full conjugated linker-CdSe-linker sequence, with two terminal carboxylate-CdSe layers according to the sequence PAAH-CdSe-(linker-CdSe-linker)($n-2$)-CdSe-SA.

The change of NCs packing during multilayers build-up (see the above reported considerations on thickness analysis) is supposed to favor the exciton delocalization described by the proposed model as an extended conjugation and a statistical contribution.

It is important to underline that the conjugative or the statistical contribution in the exciton delocalization depends on the properties of the employed S-linkers. In fact, taking into account that by exchanging CdSe-NCs native ligands with linkers whose frontier orbitals have both the energy and the symmetry that matches with NCs delocalized orbitals, it is possible to decrease the energetic barrier at the interfacial region and favor the tunneling of the excitonic charge carriers through it. In other words, if a linker possesses frontier orbital energies that are near-resonant with the band-edges of NCs core, may exist the possibility that, upon coordination with NCs, the ligand could act as a charge carriers delocalizer. In particular, treatment of NCs films with short organic or inorganic ligands proved to potentially induce exciton delocalization by enabling inter-NCs coupling and enhancing film conductivity³⁴.

In fact, we found that PDTC-based multilayers have a $\Delta E_{g\infty n}$ of 48 meV (Table 2), that means an increase of the exciton delocalization of 0.59 nm. This result is also supported by previous reported theoretical calculations³. They have shown that the dithiocarbamate causes hybridization of the PDTC HOMO state with the CdSe-NCs layers, favouring charge delocalization over two layers, first step to have a good photoconductor layer as the PDTC-based multi-layered system is reported to be². On the other hand, $\Delta E_{g\infty n}$ for EDTC-based multilayers is 30 meV lower than the one of PDTC-based ones (Table 2) with an apparent increase of the exciton radius of just 0.2 nm. Again, reported theoretical calculations³, show that hybridization involves only the dithiocarbamate anchoring group of

EDTC and it is localized at the proximity of the interface linker/CdSe-NCs. In this case the EDTC-based multilayer results to be a worse photoconductor compared the PDTC one². TTTP-based multilayers have a $\Delta E_{g\infty}$ and ΔR comparable with the one of EDTC-based ones (Table 2), that combined with the very low photoconductivity is in agreement with the idea that a low ΔR corresponds at a lower possibility to have charge transfer between NCs layers.

So it seems, so far, that a $\Delta E_{g\infty n}$ corresponds to good photoconductivity properties and vice versa. This is in principle true, because the delocalization of the NCs exciton along the linker or on different NCs is the first step to have charge transport, however it is not the only aspect that we have to take into account. For example, sulphide ion-based multilayers have a $\Delta E_{g\infty}$ (66 meV) higher than the other S-linkers-based multilayers (Table 2), corresponding of a ΔR of 0.85 nm. However, the multilayers show photocurrents that are 10-times lower than PDTC-based ones and comparable with PAAH-based multilayers. We explain this result with the formation of a CdS shell on the CdSe-NCs surface as above described for monolayers. Unfortunately, the reported band-edges of CdS, do not match with the ones of CdSe-NCs³⁵, so, the unexpected low photoconductivity responses of the multilayers, in spite of the sulphide-ion atomic dimensions and the favorable $\Delta E_{g\infty}$ value, may be ascribed to band edge misalignment.

CONCLUSIONS

The present investigation shows that sulfur-based bi-dentate ligands tetrathioterephthalate (TTTP) and sulphide dianions form regular multilayers with CdSe-NCs on ITO glass via layer-by-layer alternation.

Multilayers formation produces a progressive decrease of NCs band-edge energy with the increasing number of layers n . The change of NCs packing during multilayers build-up is supposed to favor the exciton delocalization.

By modeling the dependence of the energy with n as an extended conjugation in a one-dimensional case, it was found that the relationship holds for $n > 2$. The observed energy changes could be ascribed both to an extended conjugation and to a statistical contribution. The prevalence of the conjugative or statistical contribution in the exciton delocalization depends on the characteristics of the sulfur-based bi-dentate ligands. We described the red shift as a progressive increase of the excitonic radius respect the NCs with the native ligands and we found a maximum value of 0.85 nm for the sulphide ion-based systems.

To the best of our knowledge this is the first evaluation of the progressive exciton delocalization through solid-state multilayered systems obtained by the alternation of semiconductor NCs and organic bi-dentate linkers.

EXPERIMENTAL METHODS

Chemicals and Reagents. Disodium 1,2-ethylenebis-(dithiocarbamate) (EDTC), 1,4-benzenedicarboxylic acid (TP), poly(acrylic acid) (PAAH), Na₂S and all other chemicals were reagent grade and used as received. Tetrathioterephthalate (TTTP) and 1,4-phenylenebis-(dithiocarbamate) (PDTC) were prepared as tetrabutylammonium (TBA) salts according to literature^{36,37}. Soluble CdSe-NCs with the surface capped by native ligands hexadecylamine and stearic acid were produced as previously reported²². The NCs display an absorption maximum at 597 nm corresponding to an average size of 4.5 nm³¹.

Substrates and Multilayer Film Formation. Transparent conducting surfaces ($1 \times 4 \text{ cm}^2$) were prepared from indium-tin oxide (ITO)/glass ($80 \Omega \text{ sq}^{-1}$ from Kintec, Hong-Kong). Multilayers build up was performed as previously described²² by alternatively dipping the ITO/glass substrates (coated with a PAAH monolayer from a 10^{-3} M solution of PAAH in EtOH²) into the solutions of both CdSe-NCs and the linkers. After each immersion step the substrate was carefully washed and dried in air. The exposing time was 5 min and adsorption occurs equally on both sides of the ITO/glass substrate. CdSe-NCs were used ca 0.1% by weight (ca. $5 \times 10^{-3} \text{ M}$ in CdSe units) in CHCl₃. Linkers solutions were 10^{-3} M in EtOH (TTTP) and in MeOH (EDTC, PDTC and TP). Na₂S solutions were 10^{-2} M in 1:4 v/v water/MeOH mixture.

Apparatus and Procedure. Electrochemistry was performed at room temperature in acetonitrile under nitrogen in three electrode cells. The counter electrode was platinum; reference electrode was Ag/Ag+ (0.1 M AgNO₃ in acetonitrile, 0.34 V vs SCE, -4.77 V vs vacuum), supporting electrolyte was 0.1 M tetrabutylammonium perchlorate (TBAP). The voltammetric apparatus was Metrohm Autolab 128N potentiostat/galvanostat. Working electrodes were glassy carbon (GC 0.2 cm²) for cyclic voltammetry (CV) determinations in solution and ITO/glass sheets (2 cm²) for monolayers. CV scan rates were 0.1 V s⁻¹ for solutions and 0.02 V s⁻¹ for monolayers.

UV-vis spectra were collected with a Perkin Elmer Lambda 35 spectrometer; FTIR spectra of KBr pellets were recorded on a Nicolet 6700 spectrometer.

Photoconductivity measurements of multilayers were performed with a special Hg electrode contacting the multilayer-covered ITO as described previously². Bias (100 mV) was applied to ITO vs Hg electrode. Illumination was performed on the back glass side of the ITO/multilayer with a 100 W halogen lamp, spotted over an area of ca 10 cm². The resulting light power, calibrated with a silicon photodiode, was $\sim 2 \text{ mWcm}^{-2}$.

ASSOCIATED CONTENT

Supporting Information

The Supporting information is available free of charge on the ACS Publications website at DOI UV-vis and FTIR spectra, Cyclic Voltammograms and PL measurements.

AUTHOR INFORMATION

Corresponding Author

*e-mail: barbara.vercelli@icmate.cnr.it; barbara.vercelli@cnr.it

*e-mail: tersilla.virgili@polimi.it

Author Contributions

The manuscript was written through contributions of all authors. / All authors have given approval to the final version of the manuscript. / ‡These authors contributed equally.

ACKNOWLEDGMENT

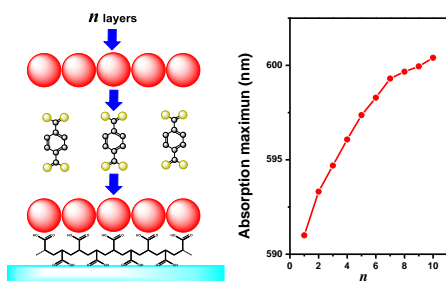
Support by the Project Accordo Quadro CNR Regione Lombardia 2016 "I-ZEB" is kindly acknowledged. We are, also, indebted with the Italian Government for the financial support-

REFERENCES

- (1) Roelofs K. E.; Brennan T. P.; Bent S. F. Interface Engineering in Inorganic-Absorber Nanostructured Solar Cells. *J. Phys. Chem. Lett.* **2014**, *5*, 348–360.
- (2) Zotti G.; Vercelli B.; Berlin A.; Virgili T. Multilayers of CdSe Nanocrystals and Bis(dithiocarbamate) Linkers Displaying Record Photoconduction. *J. Phys. Chem. C* **2012**, *116*, 25689–25693.
- (3) Virgili T.; Calzolari A.; Suárez López I.; Ruini A.; Cattellani A.; Vercelli B.; Tassone F. Hybridized Electronic States between CdSe Nanoparticles and Conjugated Organic Ligands: A Theoretical and Ultrafast Photo-Excited Carrier Dynamics Study. *Nano Res.*, **2018**, *11*, 142–150.
- (4) Zhao, Y.; Perez-Segarra, W.; Shi, Q.; Wei, A. Dithiocarbamate Assembly on Gold *J. Am. Chem. Soc.* **2005**, *127*, 7328–7329.
- (5) Xing Y.; Park T.-H.; Venkatramani R.; Keinan S.; Beratan D. N.; Therienand M. J.; Borguet E. Optimizing Single-Molecule Conductivity of Conjugated Organic Oligomers with Carbodithioate Linkers. *J. Am. Chem. Soc.* **2010**, *132*, 7946–7956.
- (6) Li Z.; Kosov D. S. Dithiocarbamate Anchoring in Molecular Wire Junctions: A First Principles Study. *J. Phys. Chem. B* **2006**, *110*, 9893–9898.
- (7) Wessels J. M.; Nothofer H.-G.; Ford W. E.; von Wrochem F.; Scholz F.; Vossmeier T.; Schroedter A.; Weller H.; Yasuda A. Optical and Electrical Properties of Three-Dimensional Interlinked Gold Nanoparticle Assemblies. *J. Am. Chem. Soc.* **2004**, *126*, 3349–3356.
- (8) Querner C.; Reiss P.; Bleuse J.; Pron A. Chelating Ligands for Nanocrystals Surface Functionalization. *J. Am. Chem. Soc.* **2004**, *126*, 11574–11582.
- (9) Neofotistou E.; Malliakas C. D.; Trikalitis P. N. Novel Coordination Polymers Based on the Tetrathioterephthalate Dianion as the Bridging Ligand. *Inorg. Chem.* **2007**, *46*, 8487–8489.
- (10) Han M. J.; Liu C. Y.; Tian P. F. Enhanced Electronic Coupling in a Molecular Pair of Dimolybdenum Units Bridged by a Tetrathioterephthalate Dianion. *Inorg. Chem.* **2009**, *48*, 6347–6349.
- (11) Zhang H.; Jang J.; Liu W.; Talapin D. V. Colloidal Nanocrystals with Inorganic Halide, Pseudohalide, and Halometallate Ligands. *ACS Nano* **2014**, *8*, 7359–7369.
- (12) Lee J. S.; Kovalenko M.V.; Huang J.; Chung D.S.; Talapin D.V. Band-like Transport, High Electron Mobility and High Photoconductivity in All-Inorganic Nanocrystal Arrays. *Nat. Nanotechnol.* **2011**, *6*, 348–352.
- (13) Nag A.; Kovalenko M. V.; Lee J.-S.; Liu W.; Spokoyny B.; Talapin D. V. Metal-free Inorganic Ligands for Colloidal Nanocrystals: S²⁻, HS⁻, Se²⁻, HSe⁻, Te²⁻, HTe⁻, TeS₃²⁻, OH⁻, and NH₂⁻ as Surface Ligands. *J. Am. Chem. Soc.* **2011**, *133*, 10612–10620.
- (14) Nag A.; Chung D. S.; Dolzhenkov D. S.; Dimitrijevic N. M.; Chattopadhyay S.; Shibata T.; Talapin D. V. Effect of Metal Ions on Photoluminescence, Charge Transport, Magnetic and Catalytic Properties of All-Inorganic Colloidal Nanocrystals and Nanocrystal Solids. *J. Am. Chem. Soc.* **2012**, *134*, 13604–13615.
- (15) Chung D. S.; Lee J.-S.; Huang J.; Nag A.; Ithurria S.; Talapin D. V. Low Voltage, Hysteresis Free, and High Mobility Transistors from All-Inorganic Colloidal Nanocrystals. *Nano Lett.* **2012**, *12*, 1813–1820.
- (16) Rodríguez-Calero G. G.; Lowe M. A.; Kiya Y.; Abruña H. D. Electrochemical and Computational Studies on the Electrocatalytic Effect of Conducting Polymers toward the Redox Reactions of Thiadiazole-Based Thiolate Compounds. *J. Phys. Chem. C* **2010**, *114*, 6169–6176.
- (17) Huang D.; Zou Y.; Jiao F.; Zhang F.; Zang Y.; Di C.; Xu W.; Zhu D. Interface-Located Photothermoelectric Effect of Organic Thermoelectric Materials in Enabling NIR Detection. *ACS Appl. Mater. Interfaces*, **2015**, *7*, 8968–8973.
- (18) Oshima K.; Shiraiishi Y.; Toshima N. Novel Nanodispersed Polymer Complex, Poly(nickel 1,1,2,2-ethenetetrathiolate): Preparation and Hybridization for n-Type of Organic Thermoelectric Materials. *Chemistry Letters*, **2015**, *44*, 1185–1187.
- (19) Sun Y.; Sheng P.; Di C.; Jiao F.; Xu W.; Qiu D.; Zhu D. Organic Thermoelectric Materials and Devices Based on p- and n-Type Poly(metal 1,1,2,2-ethenetetrathiolate)s. *Adv. Mater.* **2012**, *24*, 932–937.
- (20) Schnitzenbaumer K. J.; Labrador T.; Dukovic G. Impact of Chalcogenide Ligands on Excited State Dynamics in CdSe Quantum Dots. *J. Phys. Chem. C* **2015**, *119*, 13314–13324.
- (21) Kambhampati P. Unraveling the Structure and Dynamics of Excitons in Semiconductor Quantum Dots. *Acc. Chem. Res.* **2011**, *44*, 1–13.

- (22) Zotti G.; Vercelli B.; Berlin A.; Chin P. T. K.; Giovannella U. Self-Assembled Structures of Semiconductor Nanocrystals and Polymers for Photovoltaics. 1. CdSe Nanocrystal-Polymer Multilayers. Optical, Electrochemical, Photoelectrochemical and Photoconductive Properties. *Chem. Mater.* **2009**, *21*, 2258-2271 and references therein.
- (23) Vercelli B.; Zotti G.; Berlin A. Self-Assembled Multilayers of CdSe Nanocrystals and Hydrazine or Linear Diamines. *J. Phys. Chem. C*, **2011**, *115*, 4476-4482.
- (24) Yu W. W.; Qu L.; Guo W.; Peng X. Experimental Determination of the Extinction Coefficient of CdTe, CdSe, and CdS Nanocrystals. *Chem. Mater.* **2003**, *15*, 2854-2860.
- (25) Yun H. J.; Paik T.; Edley M. E.; Baxter J. B.; Murray C. B. Enhanced Charge Transfer Kinetics of CdSe Quantum Dot-Sensitized Solar Cell by Inorganic Ligand Exchange Treatments. *ACS Appl. Mater. Interfaces* **2014**, *6*, 3721-3728.
- (26) Liu F.; Zhu J.; Wei J.; Li Y.; Hu L.; Huang Y.; Takuya O.; Shen Q.; Toyoda T.; Zhang B.; Yao J.; Dai S. Ex Situ CdSe Quantum Dot-Sensitized Solar Cells Employing Inorganic Ligand Exchange To Boost Efficiency. *J. Phys. Chem. C* **2014**, *118*, 214-222.
- (27) Frederick M. T.; Weiss E. A. Relaxation of Exciton Confinement in CdSe Quantum Dots by Modification with a Conjugated Dithiocarbamate Ligand. *ACS Nano* **2010**, *4*, 3195-3200.
- (28) Frederick M. T.; Amin V. A.; Swenson N. K.; Ho A. Y.; Weiss E. A. Control of Exciton Confinement in Quantum Dot-Organic Complexes through Energetic Alignment of Interfacial Orbitals. *Nano Lett.* **2013**, *13*, 287-292.
- (29) Lian S.; Weinberg D. J.; Harris R. D.; Kodaimati M. S.; Weiss E. A. Subpicosecond Photoinduced Hole Transfer from a CdS Quantum Dot to a Molecular Acceptor Bound Through an Exciton-Delocalizing Ligand. *ACS Nano* **2016**, *10*, 6372-6382.
- (30) Yu W. W.; Qu L.; Guo W.; Peng X. Experimental Determination of the Extinction Coefficient of CdTe, CdSe, and CdS Nanocrystals. *Chem. Mater.* **2003**, *15*, 2854-2860.
- (31) Bredas J. L.; Silbey R.; Boudreaux D. S.; Chance R. R. Chain-length Dependence of Electronic and Electrochemical Properties of Conjugated Systems: Polyacetylene, Polyphenylene, Polythiophene, and Polypyrrole. *J. Am. Chem. Soc.*, **1983**, *105*, 6555-6559.
- (32) Liu H.; Neal A. T.; Zhu Z.; Luo Z.; Xu X.; Tománek D.; Ye P. D. Phosphorene: An Unexplored 2D Semiconductor with a High Hole Mobility. *ACS Nano* **2014**, *8*, 4033-4041.
- (33) Woomer A. H.; Farnsworth T. W.; Hu J.; Wells R. A.; Donley C. L.; Warren S. C. Phosphorene: Synthesis, Scale-Up, and Quantitative Optical Spectroscopy. *ACS Nano*, **2015**, *9*, 8869-8884.
- (34) Kagan C. R.; Murray C. B. Charge Transport in Strongly Coupled Quantum Dot Solids. *Nat. Nanotechnol.* **2015**, *10*, 1013-1026.
- (35) Kocovski V.; Ruzs J.; Eriksson O.; Sarma D.D. First-Principles Study of the Influence of Different Interfaces and Core Types on the Properties of CdSe/CdS Core-Shell Nanocrystals. *Sci. Rep.* **2015**, 1-12.
- (36) Paital, A. R.; Zhan, J.; Kim, R. H.; Kampf, J.; Collins, P.; Coucouvanis, D. Synthesis and Structures of Perthio-and Polymeric Metal Complexes with the Tetrathio-and Dithioterephthalate ligands. *Polyhedron*, **2013**, *64*, 328-338.
- (37) Daisuke A.; Sasanuma Y. Molecular Design, Synthesis and Characterization of Aromatic Polythioester and Polydithioester. *Polym. Chem.* **2012**, *3*, 1576-1587.

TOC Graphic



Multilayers of Carbodithioate and Sulfide-Linked CdSe Nanocrystals: Progressive Increasing of Exciton Delocalization

B. Vercelli ^{a*}, T. Virgili^{*b}, M. Pasini^c, A. Berlin^d, G. Zotti^e

^aIstituto di Chimica della Materia Condensata e di Tecnologie per l'Energia – CNR-ICMATE
Milano, Via Cozzi, 54 – 20125 Milano (Italy).

^bIstituto di Fotonica e Nanotecnologie – CNR-IFN, P.zza Leonardo da Vinci, 32 – 20132 Milano
(Italy).

^cIstituto per lo Studio delle Macromolecole – CNR-ISMAL, Via Alfonso Corti, 12 – 20133 Milano
(Italy).

^dIstituto di Scienze e Tecnologie Molecolari – CNR-ISTM, Via Golgi 19 – 20133 Milano (Italy).

^eIstituto di Chimica della Materia Condensata e di Tecnologie per l'Energia– CNR-ICMATE, C.so
Stati Uniti, 4 – 27135 Padova (Italy).

Exciton delocalization in multilayers

In multilayers the dependence of the energy gap (E_{gn}) vs the number of layer n could be modeled following the approach of the particle-in-a-box. By assuming that the sequence of NCs-linker subunits constitute a mono-dimensional box with an extended conjugation, like the chain length in polyconjugated systems, (E_{gn}) vs n could be modeled as follows:

$$E_{gn} = A + \frac{B}{n} \quad (1)$$

where A is the energy gap at the infinite layer ($E_{g\infty}$), while B is proportional to A as follows (see table 2 in the paper):

$$B = kA \text{ or } B = kE_{g\infty} \quad (2)$$

So equation (1) become:

$$E_{gn} = E_{g\infty} + \frac{kE_{g\infty}}{n} \quad (3)$$

We could define the energy shift at the infinite layer as

$$\Delta E_{g\infty} = E_{NC} - E_{g\infty} \quad (4)$$

where E_{NC} is the energy gap of the CdSe-NCs in solution. Equation (3) may be written as:

$$E_{gn} = E_{NC} - \Delta E_{g\infty} + \frac{k\Delta E_{g\infty}}{n} \quad (5)$$

which resembles the multilayer power-law equation (see equation (6) in footnote¹).

¹ Multilayer Power-Law

The power-law model yields a band gap of the N^{th} layer as

$$E_{gN} = \frac{E_{g1} - E_{g\infty}}{N^x} + E_{g\infty} \quad (6)$$

where E_{g1} is the band gap of the monolayer, $E_{g\infty}$ is the band gap of the bulk material and x is the parameter describing the nature of the quantum confinement in the system. x values are always comprised between 0 and 2, where the variation is in large part ascribed to the extent of the Coulomb interactions and depending on the material geometry (i. e. quantum dot vs nanowire vs 2D flake). In the case of phosphorene-based layers x exponent of equation (5) has a theoretical value of 1.0 and an experimental one comprised between 0.7 and 1.0.

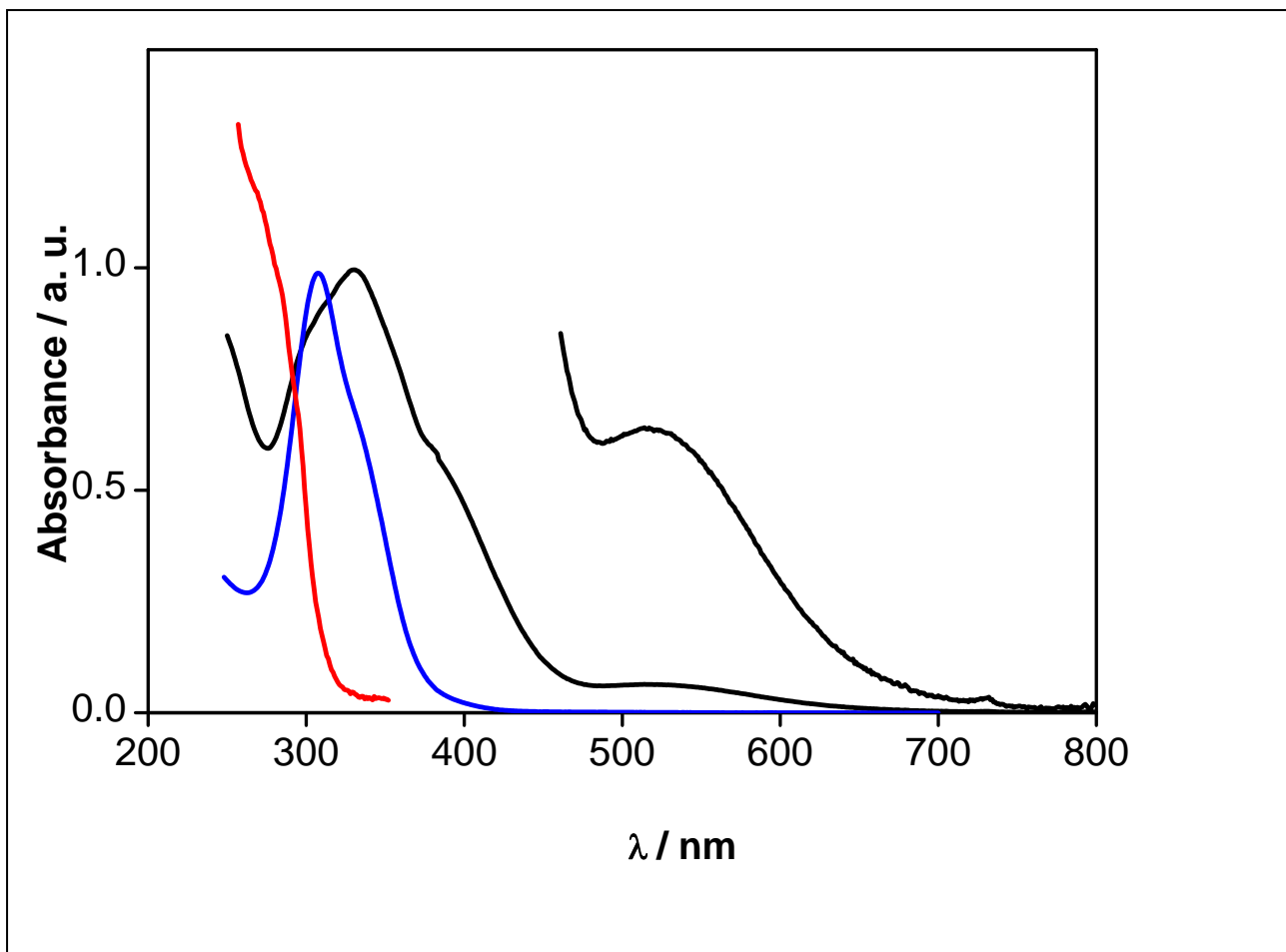


Figure S1 – Normalized electronic absorption spectra in acetonitrile of TTTP with a ten-fold magnification of its 530 nm peak (black line), PDTC (blue line) and TP (red-line).

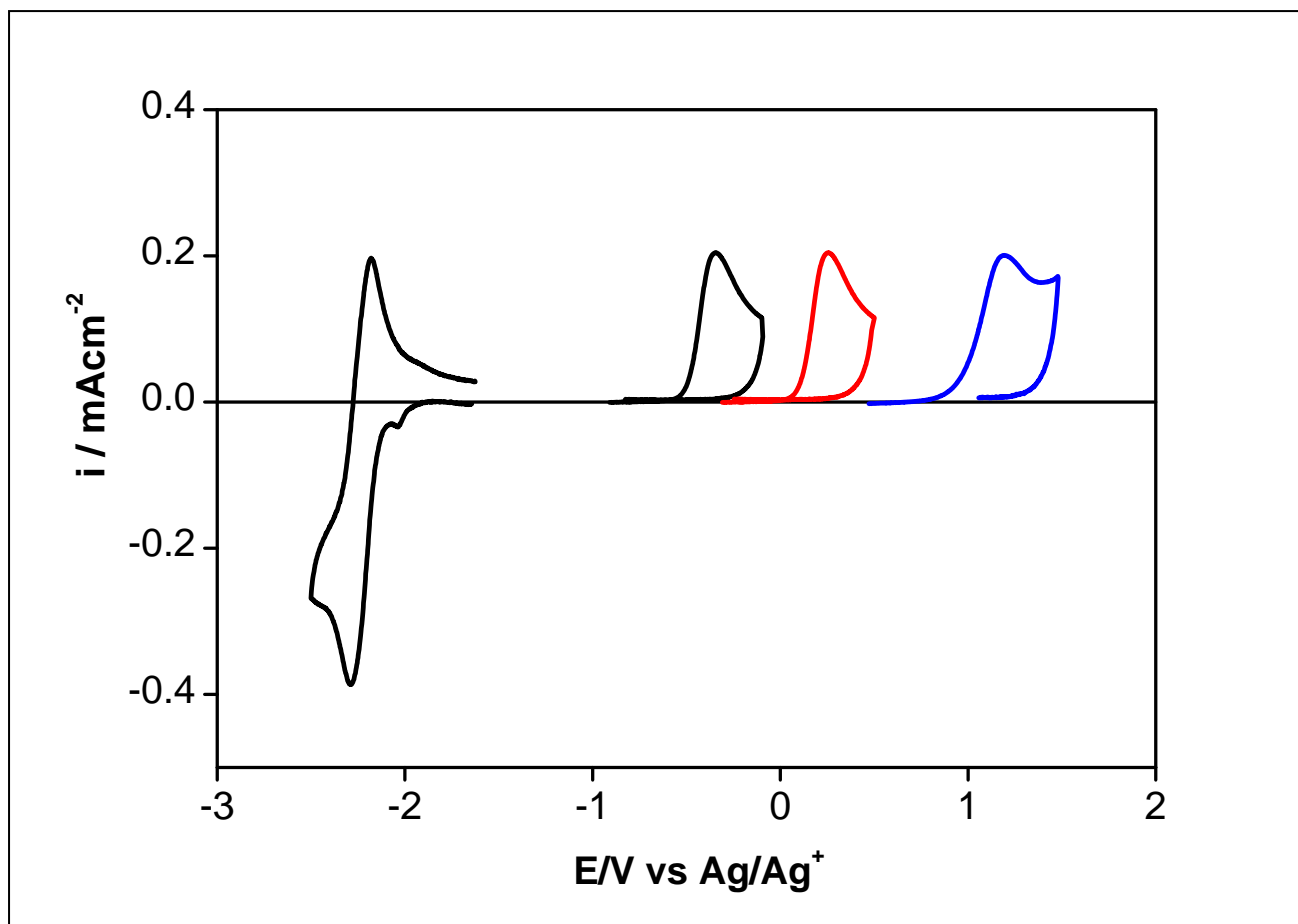


Figure S2 – Cyclic voltammograms in acetonitrile + 0.1 M TBAP of TTTP (black line), PDTC (blue line) and EDTC (red line); 10^{-3} M. GC (0.2 cm^2), $v = 0.1 \text{ V s}^{-1}$.

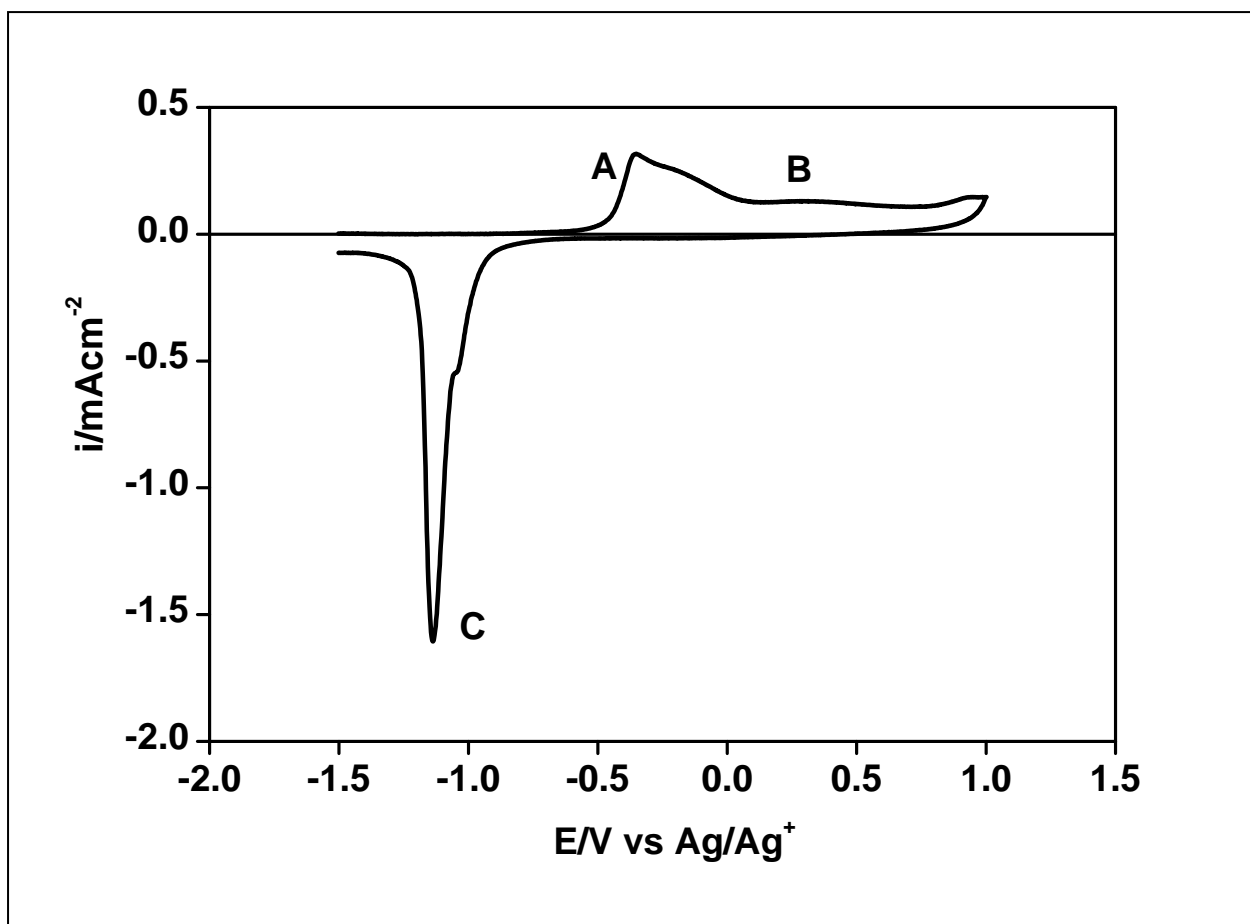


Figure S3 – Cyclic voltammograms in acetonitrile + 0.1 M TBAP of TTP

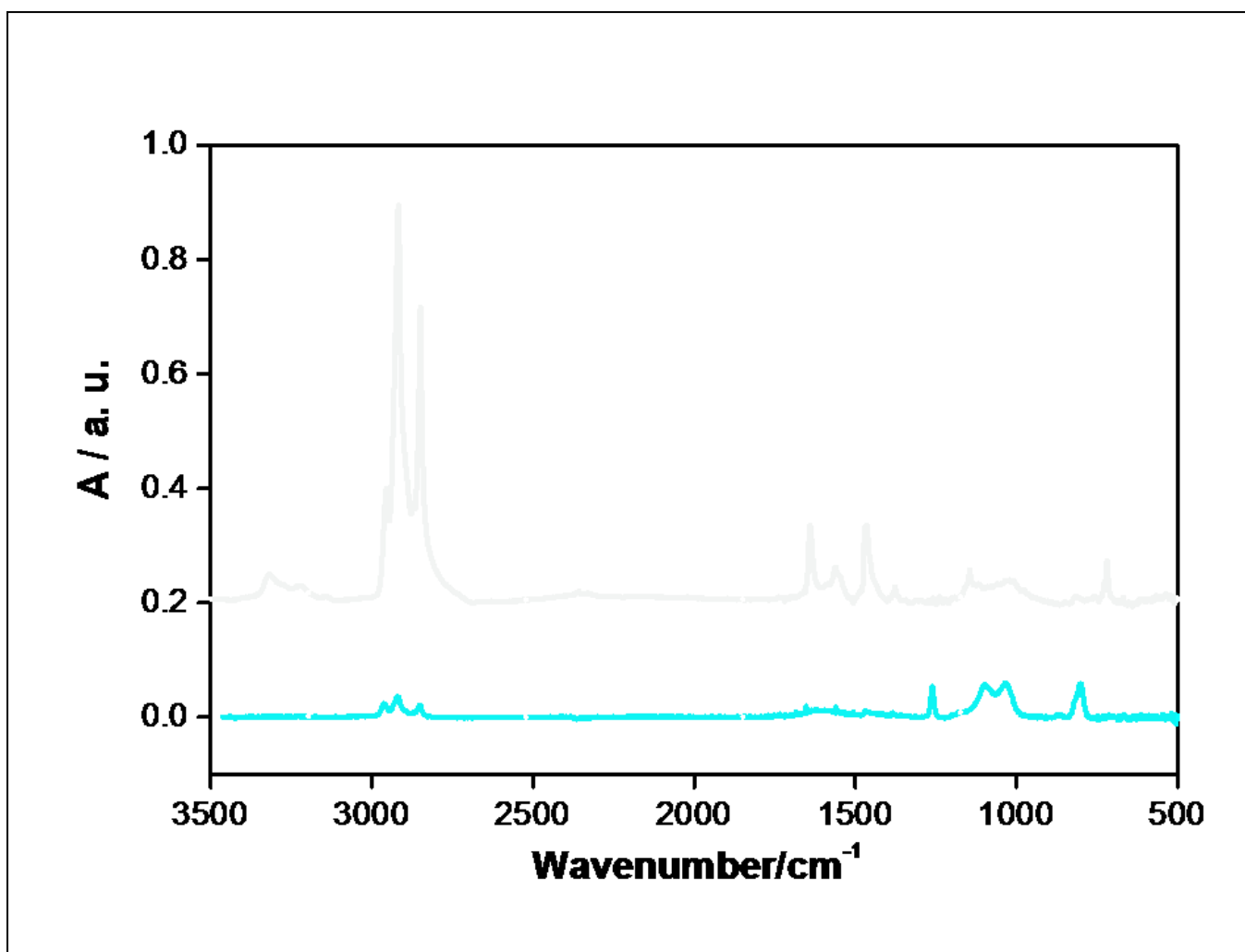


Figure S4 – FT-IR spectra in KBr of CdSe-NCs capped with native ligands (CdSe-NL, black line) and after coordination with sulfide ion (CdSe-S, red-line).

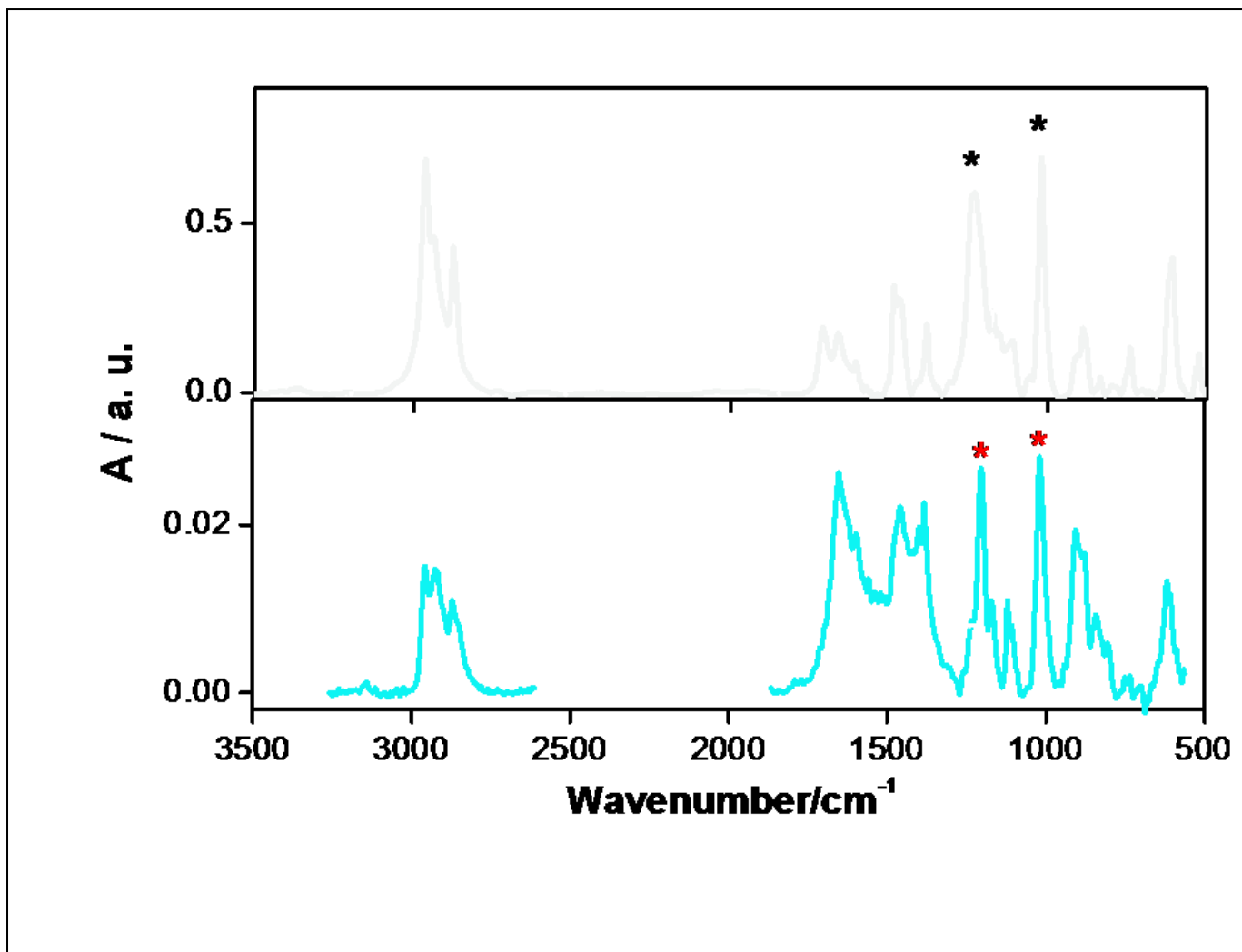


Figure S5 – FT-IR spectra in KBr of TTTP salt (black line) and after coordination with CdSe-NCs (CdSe-TTTP, red-line). C=S stretching (asym. and sym.) are starred.

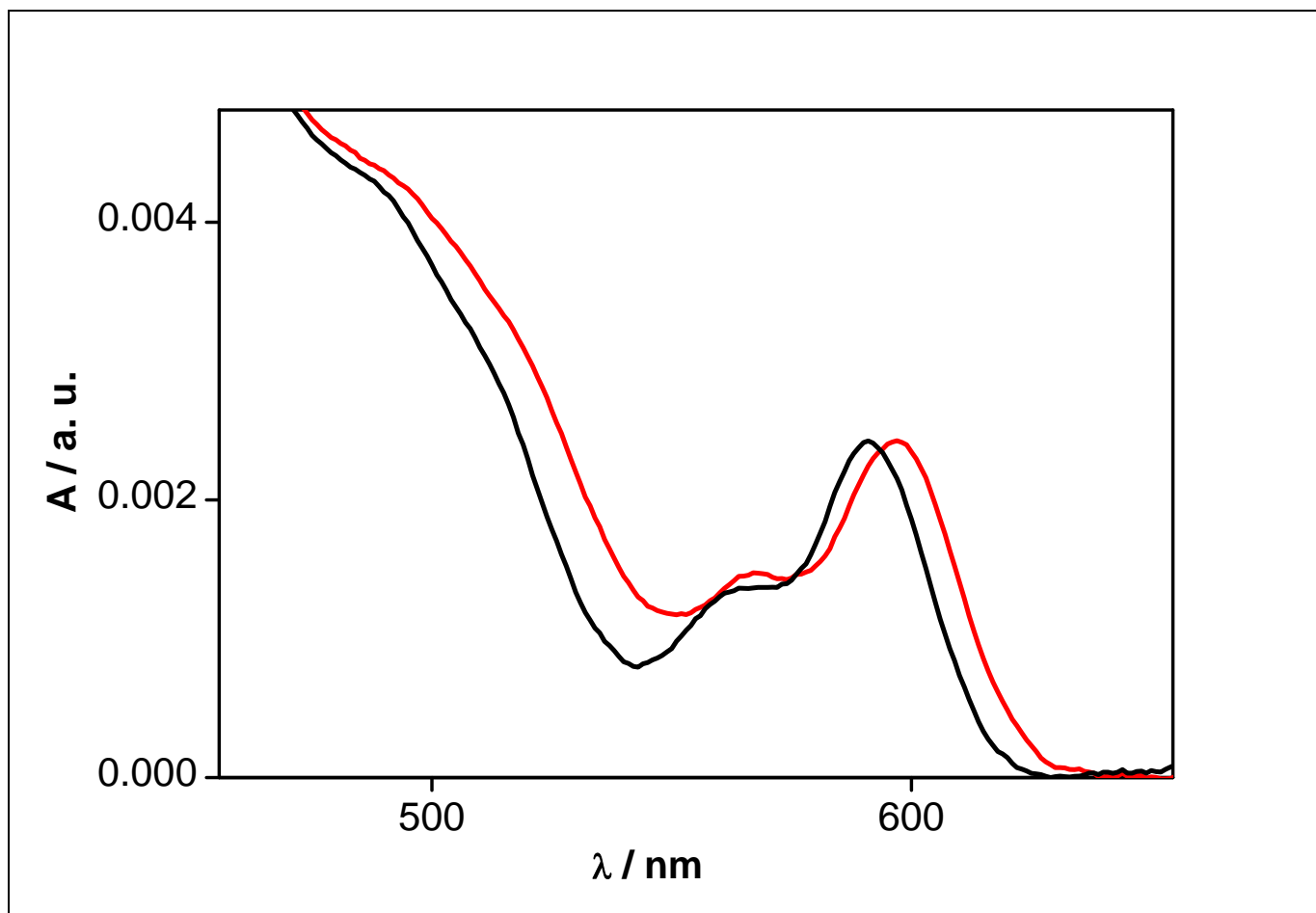


Figure S6 – UV-vis absorption spectra of CdSe-NCs monolayer with: external native ligands (black line) and sulphide ion coordinated (red line).

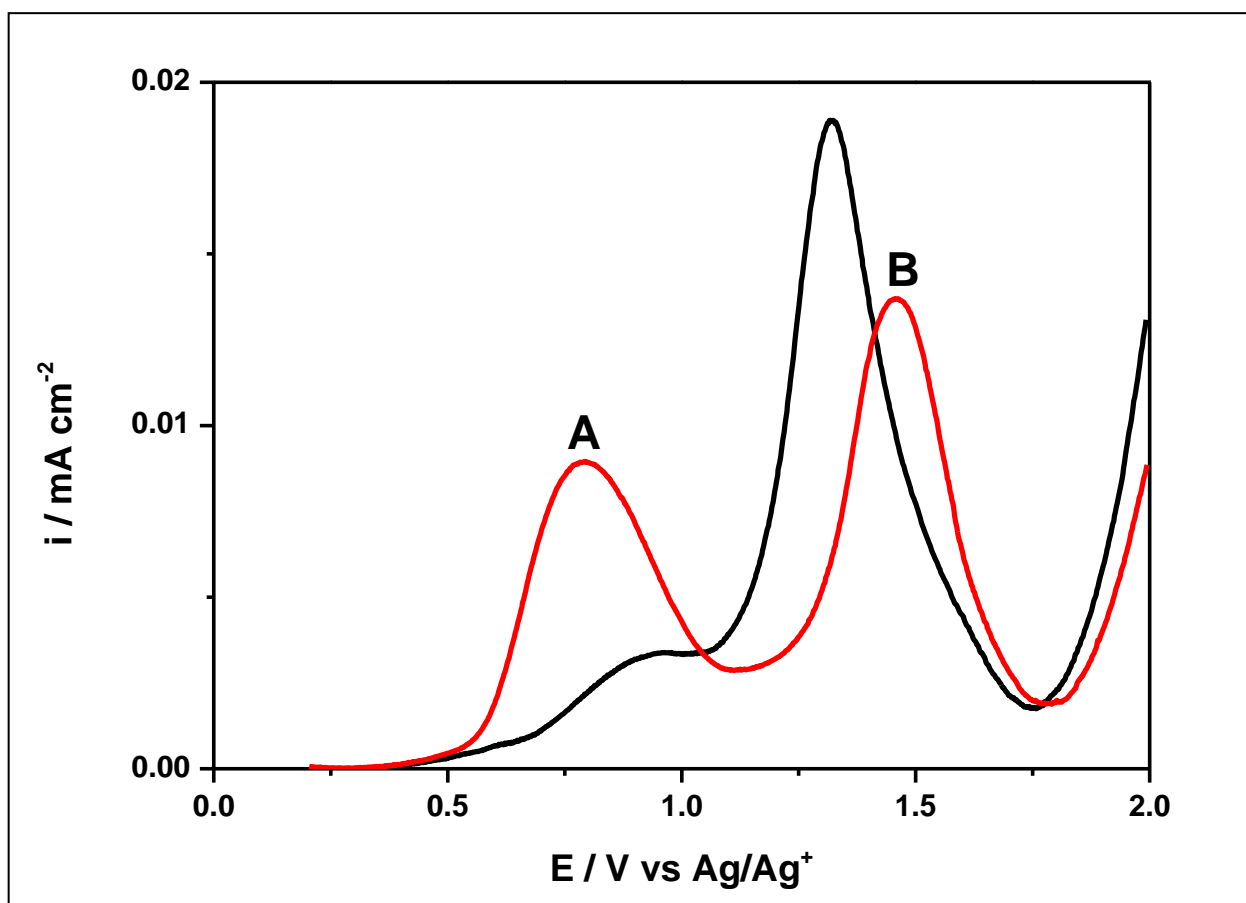


Figure S7 – Cyclic voltammograms in acetonitrile + 0.1 M TBAP of CdSe-NL before (black line) and after (red line) EtOH treatment. ITO (2 cm^2), $\nu = 0.02 \text{ V s}^{-1}$.

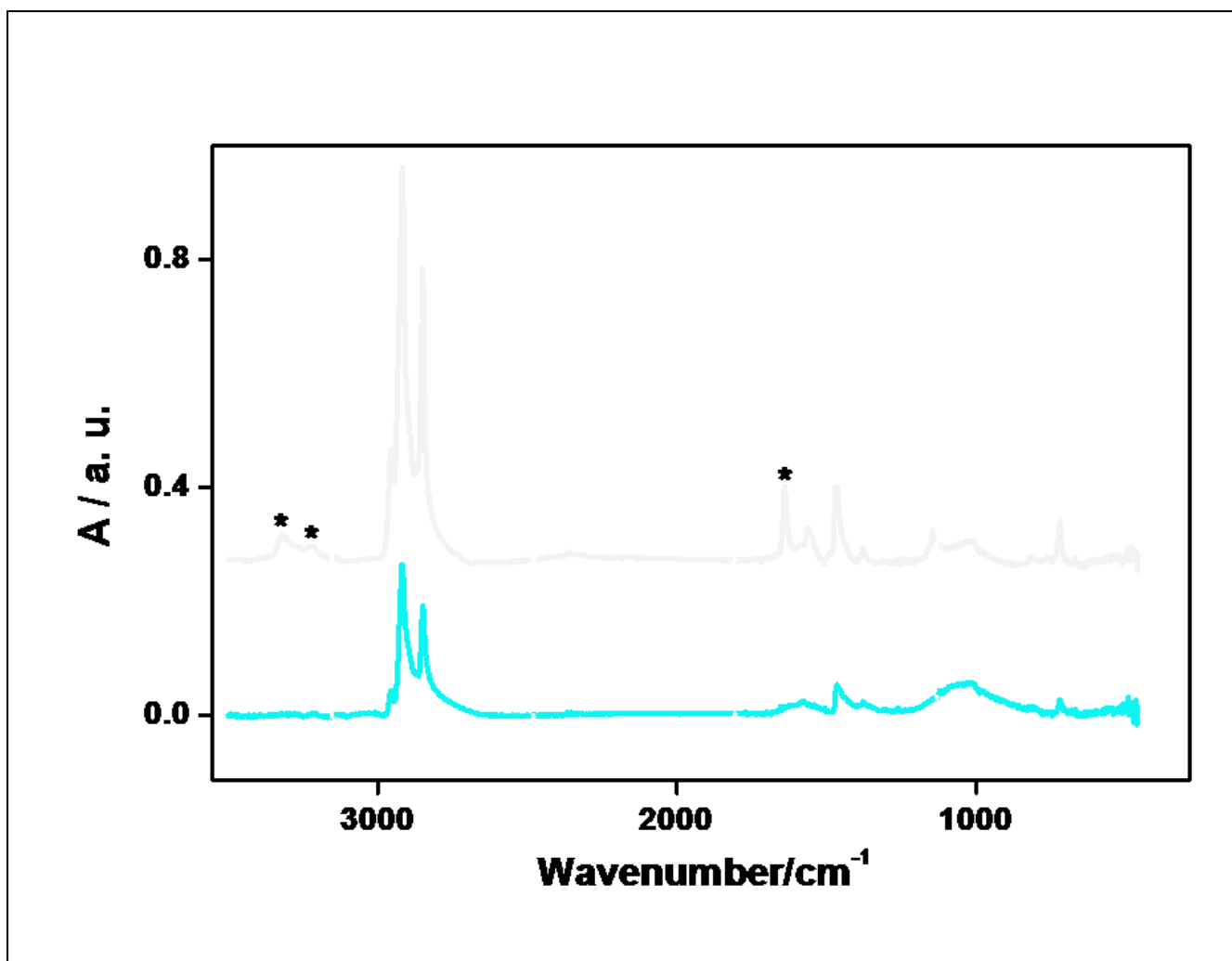


Figure S8 – FT-IR spectra in KBr of CdSe-NCs before (black line) and after (red line) EtOH treatment. HDA bands are starred.

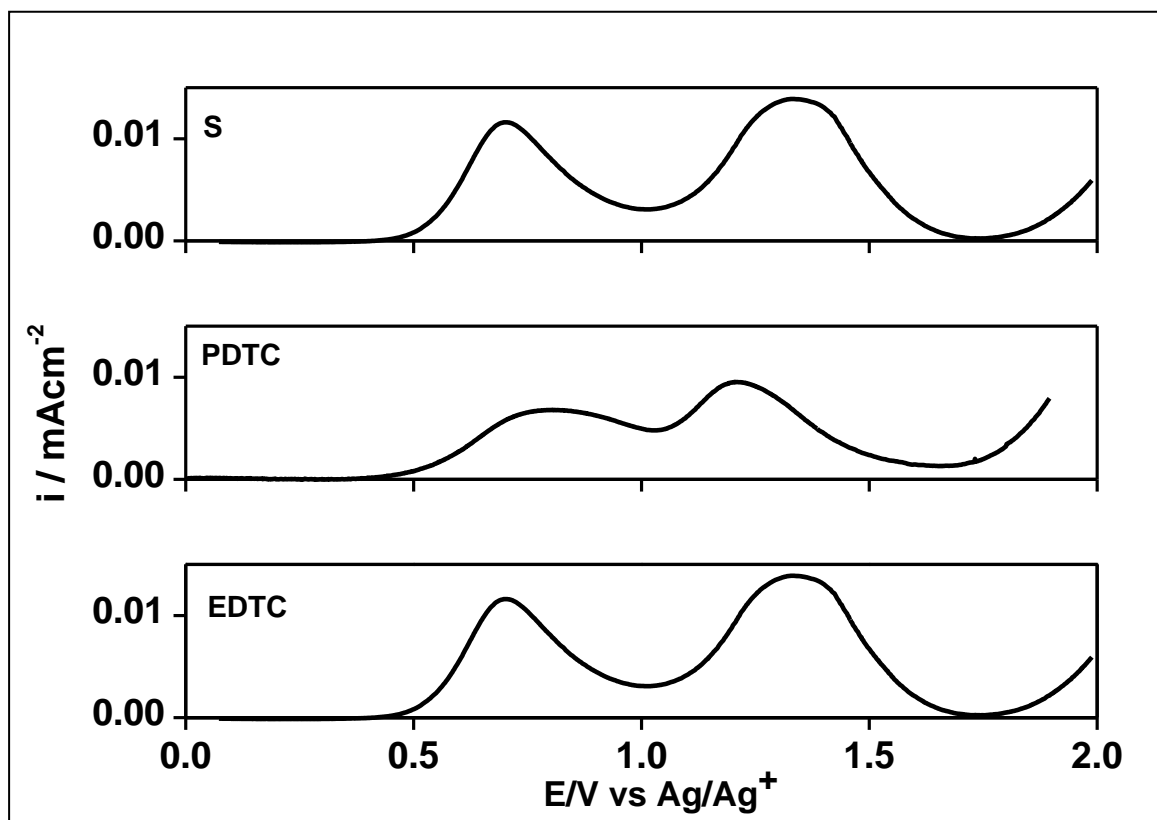


Figure S9 – Cyclic voltammograms in acetonitrile + 0.1 M TBAP of CdSe monolayers upon coordination with sulfide, PDTC and EDTC linkers. ITO (2 cm²), $\nu = 0.02 \text{ V s}^{-1}$.

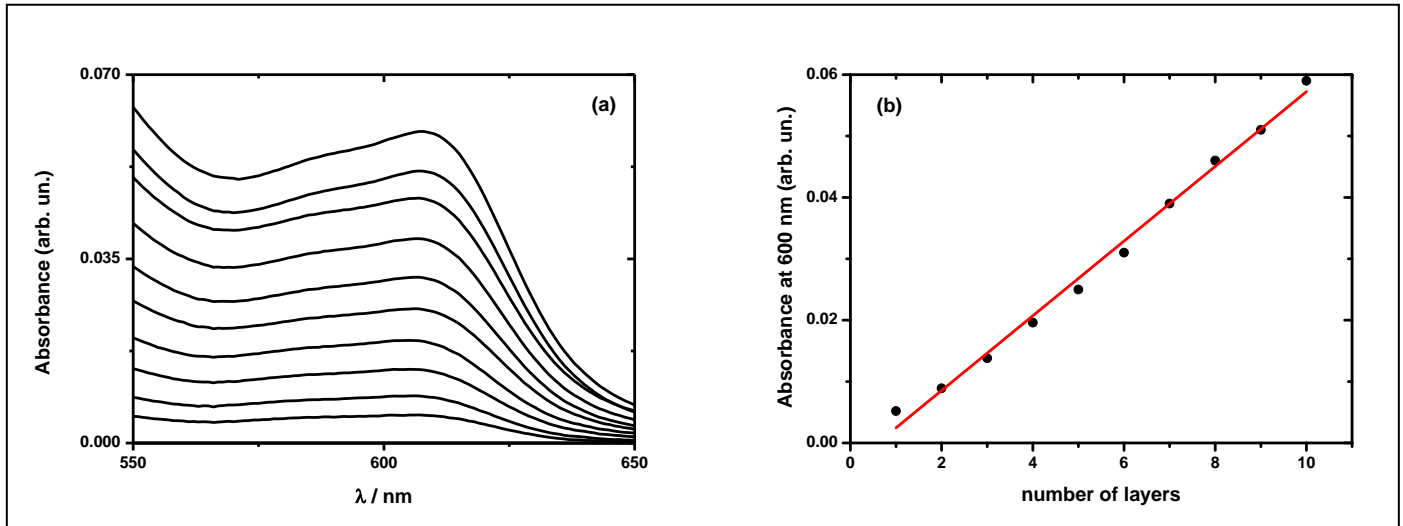


Figure S10. – (a) UV-vis spectra of ITO/PAAH/(CdSe/TP)_{n-1}/CdSe (CdSe-TP) multilayers (n = 1-10) and (b) CdSe absorbance value (at 600 nm) vs number of layers. Spectra are background normalized.

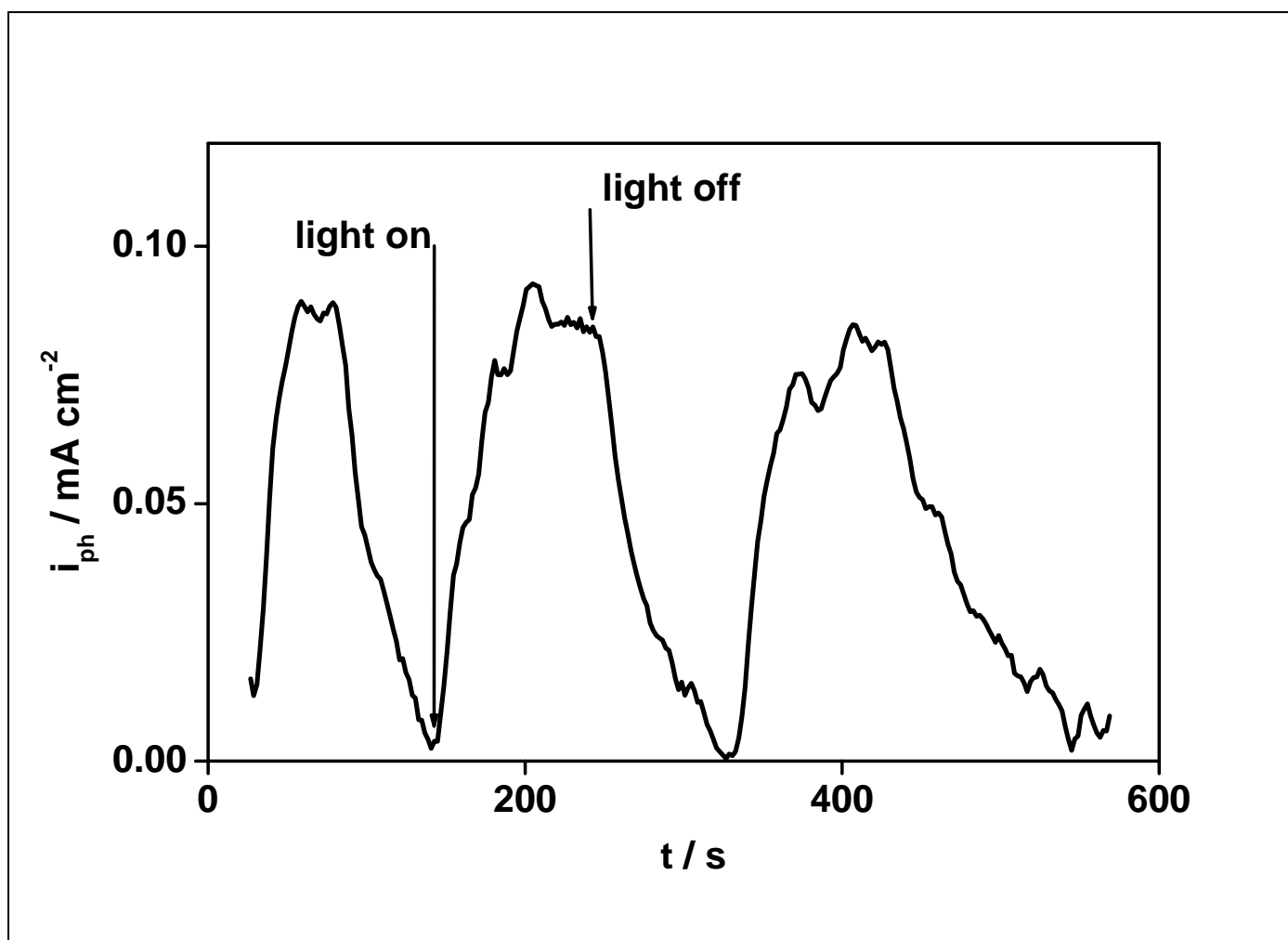


Figure S11 - Solid-state photocurrent transient of ITO/(CdSe/S)₁₀ multilayers at 100 mV applied voltage and 2 mW cm⁻² illumination.

PL Spectroscopy

Experimental

Photoluminescence experiments were carried out at room temperature. The sample was optically pumped by the second harmonic (400 nm, duration pulse of around 50 fs) of a Ti:sapphire femtosecond laser system. The incident pulse energy was ca 1 mJ. A fiber bundle was placed close to the sample to collect the emitted light. Detection was performed using an Oriel Instaspec IV spectrometer with 1 nm spectral resolution.

Results and discussion

The 10-multilayered CdSe-NCs films employed for PL determinations are sufficiently thick to avoid the quenching of the PL-signal observed in thinner CdSe-NCs layered films and ascribed to the fast electron transfer (< 1 ns) from the first monolayer toward ITO surface¹. Surprisingly, TTTP-based multilayers show a PL response (Fig. SI10), whereas TTTP dianion in EtOH solutions doesn't present any appreciable PL-signal. PL emission is at the same wavelength of CdSe-NCs absorption (Fig. SI10), suggesting that only the inorganic component of the multilayer is involved. This unexpected signal may be ascribed to a slow charge transfer among NCs. Sulphide-based multilayers do not give any appreciable PL response. In fact, reported data on dispersions of CdSe-NCs capped with hydrogen sulphide or sulphide-ion linkers^{13main text} suggest that they retained their band-edge PL, because they do not possess midgap states serving as fast non-radiative recombination channels. These considerations support the idea that PL quenching in sulphide-based multilayers is due to exciton delocalization beyond the NCs radius. Reported data on EDTC and PDTC linkers^{2 main text}, show the dithiocarbamate anchoring groups quenching effect on PL. In particular in PDTC-based multilayers PL is almost totally suppressed.

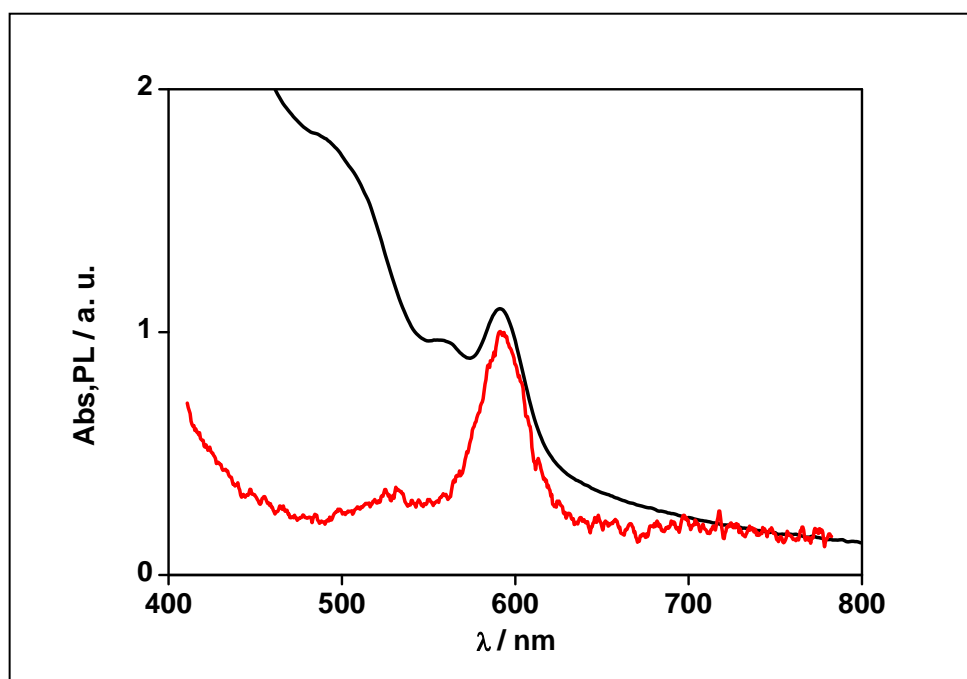


Figure S12. – Adsorption (black line) and Photoluminescence (red line) spectra of ITO/(CdSe/TTTP)₁₀ multilayered films.

References

[1] Zillner E., Fengler S., Niyamakom P., Rauscher F., Köhler K., Dittrich T., Role of Ligand Exchange at CdSe Quantum Dot Layers for Charge Separation, *J. Phys. Chem. C* **2012**, 116, 16747.